Time-Resolved Charge Carrier Generation from Higher Lying Excited States in Conjugated Polymers

C. Gadermaier,[1,2,*] G. Cerullo,[1] G. Sansone,[1] G. Leising,[3] U. Scherf,[4] and G. Lanzani[1]

[1]*Dipartimento di Fisica, Politecnico di Milano, Piazza Leonardo da Vinci 32, 20133 Milano, Italy*

[2]*Institut für Festkörperphysik, Technische Universität Graz, Petersgasse 16, 8010 Graz, Austria*

[3]*Science & Technology, AT&S AG, Fabriksgasse 13, 8700 Leoben, Austria*

[4]*Institut für Physikalische Chemie und Theoretische Chemie, Universität Potsdam, Karl-Liebknecht-Straße 24-25, 14476 Golm, Germany*

(Received 18 January 2002; published 26 August 2002)

Sub-ps three-pulse transient differential transmission spectroscopy using two excitation pulses is used to directly investigate the generation of charge carriers in ladder-type poly(*para*)phenyl in bulk film. The role of higher excited singlet states of both even and odd symmetry is examined and the dynamics of the major processes involved is described quantitatively. The charge generation efficiency is found to depend strongly on the delay between the two excitation pulses. This is explained by the interplay between internal conversion, excitation energy migration, and on-site vibronic relaxation.

DOI: 10.1103/PhysRevLett.89.117402 PACS numbers: 78.47.+p, 78.66.Qn

π-conjugated polymers find rapidly growing application in organic light emitting diodes (OLEDs) [1] and lasers [2], and have a high potential for other uses, such as photovoltaics (PV) and photodetectors (PD) [3]. Nonequilibrium, hot states generated by charge coalescence in OLEDs, by optical absorption in PVs or PDs, by sequential excitation [4], or by exciton mutual interaction at high excitation density (notably in lasers) are the primary excitations involved in the fundamental processes of device operation. From such states charge carrier generation (CG) may take place. CG is the basic step in PV or PD, while it lowers the efficiency of OLEDs and lasers. In the molecular solid picture, it is explained by dissociation of the first excited neutral photoexcitations during energy relaxation [5]. Frolov *et al.* [6,7] have found evidence for CG from singlet states higher than the lowest excited singlet state S_1 in PPV. Theoretical modeling suggests that higher excited states may have a higher dissociation probability due to their peculiar electron distribution [8].

Energy relaxation mechanisms in polymer films are internal conversion, on-site vibrational relaxation (OVR) [9], and intersite excitation energy migration (EEM) [10–12]. All these processes have been invoked to model the CG mechanism, which is increasingly efficient with higher excitation energy. Dissociation via electron tunneling is favored in vibrationally hot S_1 states [13]. The disordered film is thought to contain a certain number of quenching sites which favor dissociation and can be encountered by the migrating S_1 states. This explanation is consistent with the similarity in the dynamics of CG and EEM in field-assisted pump-probe [12,14] as well as photocurrent cross-correlation measurements [15].

In this work, we directly monitor CG from higher lying states; to this purpose, we use a variant of the pump-probe technique, in which a third, ''push'' pulse is introduced between pump and probe to reexcite the system [6,7,16]. The results of this study highlight the interplay between higher lying states, internal conversion, and energy relaxation processes during CG in conjugated polymers. We study methyl-substituted ladder-type poly(para)phenyl (*m*-LPPP), one of the best characterized representatives of its class and one of the most promising candidates for applications [17–20].

m-LPPP films of approximately 100 nm thickness were spin-coated from solution upon glass substrates. The setup for sub-ps pulse generation is described in Ref. [10], For pump-probe measurements, the relative transmission change $\Delta T/T$ is measured by a lock-in amplifier referenced to the chopped pump beam. In the presence of a push beam, this value changes to $(\Delta T/T)_{\mathrm{push}}$. Chopping the push beam yields the push-induced variation of $\Delta T/T$, or $\Delta T^2/T = (\Delta T/T)_{\mathrm{push}} - \Delta T/T$.

The $\Delta T/T$ spectrum of *m*-LPPP for 1 ps pump-probe delay is shown in the upper inset of Fig. 1. Below 2.2 eV, the signal is negative (photoinduced absorption, PA) with a broad peak at 1.5 eV (subsequently referred to as PA_1). On the high energy tail of this feature are two peaks at 1.9 and 2.1 eV (PA_2). In previous literature [11], PA_1 has been assigned to singlet absorption S_1-S_n, and PA_2 to an overlap of PA_1 with a transition D_0-D_n of charged polaron states (doublets). Above 2.2 eV, the signal is positive with peaks at 2.3, 2.5, and 2.7 eV. The absorption edge of *m*-LPPP is 2.7 eV; hence, the 2.7 eV feature is assigned to photobleaching, while the other two are stimulated emission (SE). The main Fig. 1 compares part of the spectrum for pump-probe delays 300 and 10 ps for pump energies 3.2 and 4.8 eV, normalized to the bleaching to compensate for different excitation densities. For 4.8 eV, SE is weaker and PA_2 is stronger than for 3.2 eV.

The transient behavior of SE at 2.5 eV is displayed in Fig. 2. The initial fast decay is due to bimolecular S_1 annihilation as a consequence of the high excitation

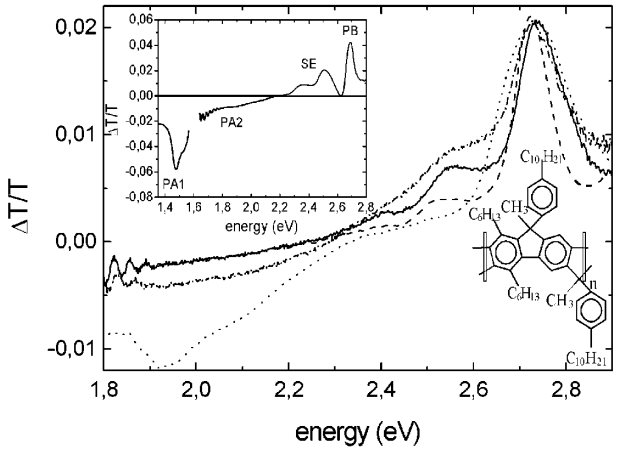

FIG. 1. Transient differential transmission spectrum of *m*-LPPP at pump-probe delays 300 fs for excitation at 3.2 eV (solid line), respectively, 4.8 eV (dash-dotted line), and 10 ps (dashed line for 3.2 eV, dotted line for 4.8 eV). Upper inset shows larger part of spectrum for 3.2 eV; lower inset shows chemical structure of *m*-LPPP.

density (8×10^{19} cm^{-3}), necessary to obtain a sufficient $\Delta^2 T/T$ signal. Upon reexcitation with a 1.6 eV pulse after 300 fs, the SE is instantaneously reduced by roughly 80%. Most of the SE recovers within less than 1 ps, but there is still a residual quenching of 7% at the end of our temporal window of 3.5 ps.

Information about the fate of the species that do not recover to the emitting state can be gained from the $\Delta^2 T/T$ spectrum, depicted in Fig. 3. In the SE region $\Delta^2 T/T < 0$, which points to a reduction of SE as in the transient dynamics. In the PA region $\Delta^2 T/T > 0$ below 1.8 eV, which corresponds to a reduction of PA_1 by depletion of the S_1 population. Above 1.8 eV, where PA_1 and PA_2 overlap $\Delta^2 T/T < 0$; the reduction of PA_1 is dominated by an increase of PA_2; the peaks at 1.9 and 2.1 eV are well resolved.

The transient $\Delta^2 T/T$ at 1.9 eV ($PA_1 + PA_2$) is shown in Fig. 4. Initially, a positive $\Delta^2 T/T$, i.e., a reduced PA is found. After roughly 300 fs, $\Delta^2 T/T$ reaches a negative value which remains fairly constant up to 40 ps. Analogously to SE, the reduction of PA_1 is instantaneous and to a large extent recovers during 1 ps; hence, the $\Delta^2 T/T$ dynamics of the PA_2 contribution (i.e., the additional absorbers created by the push beam) can be extracted: a formation time of a few hundred fs and a slow decay (see fit below).

Figure 1 shows that, for the excitation at 4.8 eV, the yield of charges is higher compared to the 3.2 eV excitation. The 4.8 eV pulse excited *m*-LPPP into a higher optically allowed state S_m ($m \neq n$, since the parities are different for one-step and two-step excitation). As already shown for poly(2-methoxy-5-(29-ethylhexyloxy)-p-phenylene vinylene) [8], it can be assumed that, from S_m, and/or during

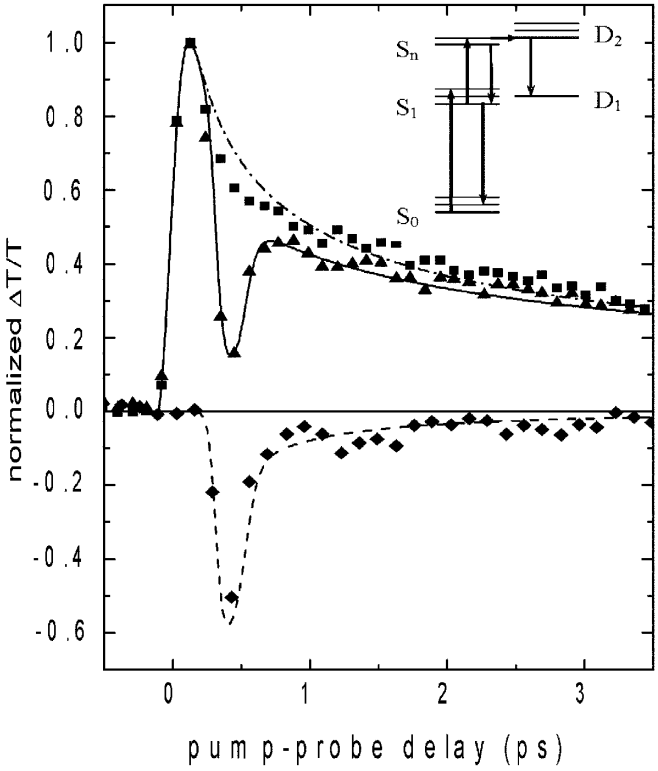

FIG. 2. Transient transmission dynamics at 2.5 eV with (triangles) and without (squares) reexcitation 300 fs after pump pulse. Diamond curve shows the difference between the two cases; lines show fit (parameters, see text). Inset shows the energy level structure of *m*-LPPP.

its vibrational relaxation, a branching into at least two paths takes place: one towards S_1 and one towards D_0.

An analogous branching can be assumed for S_n, which is reached via reexcitation of S_1. Figure 2 shows that the S_1 population is efficiently depleted towards S_n and the recovery is fast but incomplete. This is in agreement with the

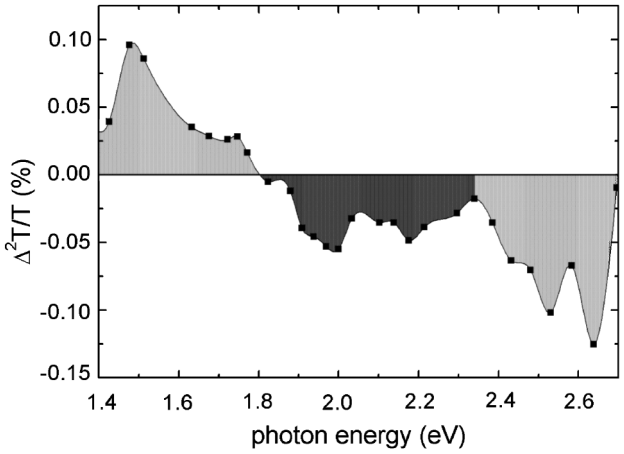

FIG. 3. Double-differential transmission spectrum of *m*-LPPP for reexcitation 300 fs after pump, probed after 10 ps.

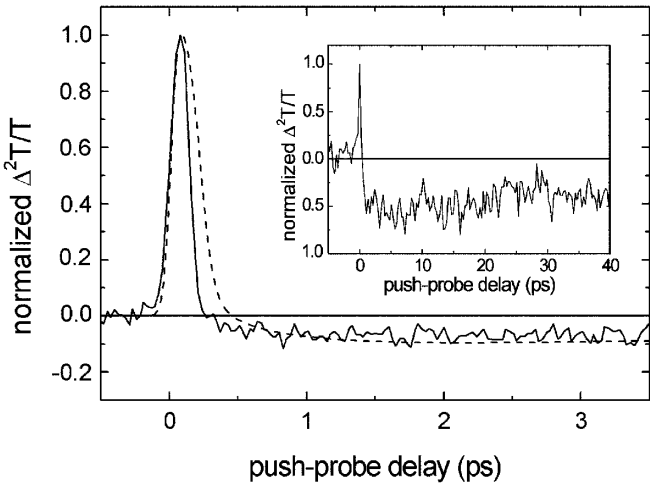

FIG. 4. Double-differential transmission dynamics at 1.9 eV for reexcitation 300 fs after pump. Dashed line shows fit as discussed in the text. Inset shows the behavior on a longer time scale.

Kasha rule [21] since the conversion from S_n is much faster than the lifetime of S_1, but indicates a breakdown of the Vavilov rule because the conversion towards S_1 does not occur with unitary efficiency. A fraction of the S_m and S_n population ends up as charge carrier pairs.

The most simple model which satisfactorily fits the temporal evolution of the S_1 population assumes Gaussian pump and push pulses [expressed as $g_1(t)$ and $g_2(t)$ in the following equations) of FWHM 180 and 150 fs, respectively [10]. As the dominant decay route of S_1, we assume a bimolecular annihilation with a Förster-type transfer resulting in a cubic dependence on the excited state concentration [4] with a rate parameter $\gamma_c = 1.2 \times 10^{-43}$ cm^3 fs^{-1}. The exponential contribution from unimolecular radiative and nonradiative decay with a comprehensive time constant of a few hundred ps (see below) is not considered for the fast processes on the displayed time scale of 3 ps. Via the push pulse S_n states are formed from S_1. From S_n, we assume two unimolecular channels with respective rates of $k_1 = 17$ ps^{-1} towards S_1 and $k_2 = 2.8$ ps^{-1} towards charge carrier pairs, according to the reaction $S_n + S_0 \rightarrow D^+ + D^-$ [which gives rise to the term $-k_2 S_n(t)$ in Eq. (3)]. Polarons decay via diffusion-mediated (quadratic) bimolecular recombination (annihilation parameter $\gamma_D = 6 \times 10^{-23}$ cm^3 fs^{-1}):

$$\frac{dS_1(t)}{dt} = g_1(t)S_0(t) - \gamma_c S_1^3(t) - g_2(t)S_1(t) + k_1 S_n(t), \tag{1}$$

$$\frac{dS_n(t)}{dt} = g_2(t)S_2(t) - (k_1 + k_2)S_n(t), \tag{2}$$

$$\frac{dS_0(t)}{dt} = -g_1(t)S_0(t) + \gamma_c S_1^3(t) - k_2 S_n(t), \tag{3}$$

$$\frac{dD(t)}{dt} = 2k_2 S_n(t) - \gamma_D D^2(t). \tag{4}$$

Note that we do not consider stimulated emission S_n-S_1 or S_1-S_0 induced by the push or pump pulses [22]. The time trace in Fig. 4, which is a weighted superposition of the singlet and polaron temporal evolution, is correctly reproduced assuming a ratio between the absorption cross sections of singlets and polarons of $\sigma_S/\sigma_P = 2.5$, in good agreement with the results of field-assisted pump-probe experiments [14].

The data are equally well reproduced, using lower annihilation constants, by adding a polaron generation mechanism from the bimolecular singlet recombination $S_1 + S_1 \rightarrow D^+ + D^-$. Fits based on diffusion-type quadratic singlet-singlet annihilation and/or exponential decay for polarons yield very similar values for k_1, k_2, and σ_S/σ_P but fail to correctly reproduce the singlet time trace of the pump-probe measurement in Fig. 2.

For the nonradiative decay from S_1 to S_0, a rate $k_{10} = 7 \times 10^{-4}$ ps^{-1} can be estimated from fluorescence lifetime and quantum yield measurements [23,24]. Within the harmonic approximation, the rate of internal conversion via vibrational modes can be obtained via the gap law [5],

$$\ln k_{nr} = 35.9 - 7.39 \times 10^{-4} \Delta E. \tag{5}$$

The constants in Eq. (5) were derived from studies on carotenoids [25]. For the S_1-S_0 ($\Delta E = 2.7$ eV) transition, this yields $k_{10} = 4 \times 10^{-4}$ ps^{-1}, which justifies the use of the carotenoid parameters as a first approximation. Using the same parameters for calculating the nonradiative S_n-S_1 ($\Delta E = 1.5$ eV) transition rate, one obtains $k_{n1} = 0.4$ ps^{-1}, which is almost 2 orders of magnitude lower than k_1. This discrepancy suggests a large anharmonicity of the molecular vibrations in the excited state geometry.

Figure 5 displays the $\Delta^2 T/T$ signal at 10 ps as a function of the pump-push delay τ_r, i.e., the time between excitation and reexcitation, and compares it to the $\Delta^2 T/T$ at 1.6 eV (essentially the population dynamics of the S_1 states). If the polaron quantum yield from the push were independent of τ_r, the number of polarons generated via reexcitation would be proportional to the number of S_1 states, and the two dynamics would be exactly the same. However, the dependence of $\Delta^2 T/T$ upon τ_r is much faster than the S_1 decay, indicating that the polaron quantum yield decreases rapidly with increasing τ_r. The time scale of this fast reduction of the S_n dissociation rate suggests that k_2 be related to the energy relaxation of S_1. Similar to the dissociation of S_1 states, this can be related to EEM and/or OVR. One can assume quenching sites which do not quench S_1 states but do quench S_n states during EEM. Since the conversion from S_n to S_1 is fast (50 fs), the

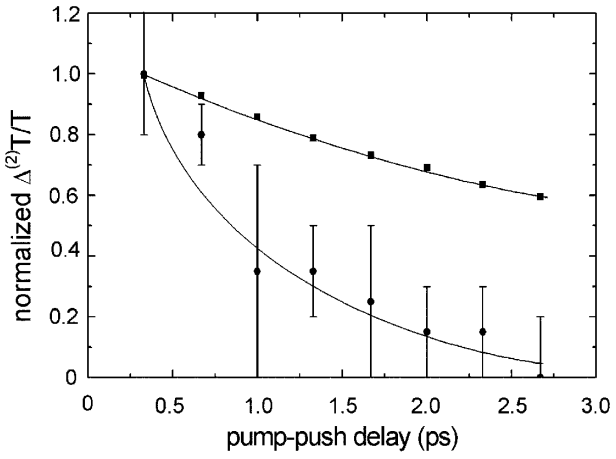

FIG. 5. Double-differential signal at 10 ps after push in function of pump-push delay (lower curve). Upper curve shows transient transmission dynamics at 1.6 eV.

migrating species is S_1, but not S_n, and therefore the dissociation of S_n is enhanced only if it is created at an S_n-quenching site. Consequently, this assumption implies that the lowest energy sites are less likely to be S_n quenching, otherwise the S_n dissociation yield would still be high after the migration.

For short times t_f after formation, the S_1 state is vibrationally hot. (In our case for an excitation energy of 3.2 eV, the excess energy is approximately 0.5 eV.) Consequently, the S_n state created via excitation of this hot S_1 has more excess energy than if it had been created with the same photon energy from a relaxed S_1, and it therefore has a higher dissociation probability p_n. The vibrational heat on a site is dissipated within a few ps, which consequently decreases p_n.

When the excitation migrates from a higher to a lower energy site, on the latter there is some vibrational energy, which increases its p_n. Therefore the decrease of p_n due to OVR is slowed down by EEM. Hence, the two processes invoked to explain our results are not mutually exclusive; on the contrary, they are closely entangled.

In conclusion, we have introduced transient pump-push-probe spectroscopy with a broadband probe as a tool to study photoexcitation dynamics in π-conjugated materials. Applying it to *m*-LPPP, we examined higher excited singlet states and found that their dynamics includes dissociation into charge carriers. When reexciting the S_1 state, we find that the charge carrier yield depends strongly on its ''age,'' which we related to the highly nonequilibrium initial configuration that relaxes to an equilibrium one over various mechanisms, which are interdependent and each contribute to charge carrier generation.

We thank M. Zavelani-Rossi, D. Polli, and E. J. W. List for their involvement in the experiments and discussion, and the CUSBO large scale facility for financial support.

*Corresponding author.
Email address: c.gadermaier@tugraz.at

[1] C. W. Tang and S. A. Van Slyke, Appl. Phys. Lett. **51**, 913 (1987).
[2] N. Tessler, G. J. Denton, and R. H. Friend, Nature (London) **382**, 695 (1996).
[3] G. Yu *et al.*, Science **270**, 1789 (1995).
[4] M. A. Stevens *et al.*, Phys. Rev. B **63**, 165213 (2001).
[5] M. Pope and C. E. Swenberg, *Electronic Processes in Organic Crystals* (Oxford University Press, New York, 1999).
[6] S. V. Frolov *et al.*, Phys. Rev. Lett. **78**, 4285 (1997).
[7] S. V. Frolov *et al.*, Phys. Rev. Lett. **85**, 2196 (2000).
[8] A. Köhler *et al.*, Nature (London) **392**, 903 (1998).
[9] A. Laubereau and W. Kaiser, Rev. Mod. Phys. **50**, 607 (1978).
[10] G. Cerullo *et al.*, Phys. Rev. B **57**, 12 806 (1998).
[11] W. Graupner *et al.*, Phys. Rev. Lett. **76**, 847 (1996).
[12] R. Kersting *et al.*, Phys. Rev. Lett. **73**, 1440 (1994).
[13] Z. D. Popovich, Chem. Phys. **86**, 311 (1984).
[14] W. Graupner *et al.*, Phys. Rev. Lett. **81**, 3259 (1998).
[15] C. Zenz *et al.*, Chem. Phys. Lett. **341**, 63 (2001); J. G. Müller *et al.*, Phys. Rev. Lett. **88**, 147401 (2002).
[16] I. B. Martini, E. R. Barthel, and B. J. Schwartz, Science **293**, 462 (2001).
[17] C. Waldauf *et al.*, Opt. Mat. **9**, 449 (1998).
[18] A. Haugeneder *et al.*, Phys. Rev. B **59**, 15 346 (1999).
[19] S. Stagira, Appl. Phys. Lett. **73**, 2860 (1998).
[20] U. Lemmer, A. Haugeneder, C. Kallinger, and J. Feldmann, in *Semiconducting Polymers*, edited by G. Hadziioanou and P. F. van Hutten (Wiley-VCH, Weinheim, 2000), p. 309.
[21] M. Kasha, Discuss. Faraday Soc. **9**, 14 (1950).
[22] The initial excited state is a vibronic replica S_n^* (S_1^*) which quickly relaxes towards zero-phonon S_n (S_1). If the lifetime τ_i of the initial S_n^* (S_1^*) were longer than the pulse duration, a depopulation exceeding 50% could not be achieved. We attempted to fit the time traces of Figs. 2 and 4, taking account of this process, satisfactorily fitting the data for $\tau_i < 20$ fs.
[23] G. Dicker *et al.*, Synth. Met. **102**, 873 (1999).
[24] J. Stampfl *et al.*, Synth. Met. **71**, 2125 (1995).
[25] P. O. Andersson and T. Gillbro, J. Chem. Phys. **103**, 2509 (1994), and references therein.